Sultan Qaboos University
Journal of Arts & Social Sciences

جامعة السلطان قابوس
مجلة الآداب والعلوم الاجتماعية

An Analysis on the Impact of Normalized Difference Vegetation Index (NDVI) Changes on the Land Surface Temperature (LST) using Satellite Imagery in the West Bank, Palestine

Ahmed Ghodieh

Associate Professor
Department of Geography
An-Najah National University
Palestine
ahmed@najah.edu

Date received: 08/01/2023
Date of acceptance: 25/04/2023

Volume (15) Issue (1), April 2024

An Analysis on the Impact of Normalized Difference Vegetation Index (NDVI) Changes on the Land Surface Temperature (LST) using Satellite Imagery in the West Bank, Palestine

Ahmed Ghodieh

Abstract

This study investigated the impact of the Normalized Difference Vegetation Index (NDVI) on the Land Surface Temperature (LST) in the West Bank, Palestine, using multitemporal satellite imagery. Landsat 5 TM and Landsat 8 OLI data were used in the study. The Landsat 5 TM data was acquired on March 29, 2001, while the Landsat 8 OLI data was acquired on April 05, 2021. The NDVI and the LST for the two images were then calculated from the two images using ArcGIS 10.8 software. Results of the study showed that the NDVI of the 2021 image was much higher than that of the 2001 image. The mean NDVI of the 2001 image was 0.25, while that of the 2021 image was 0.32. As for the LST, the mean LST of the 2001 image was 29.85 °C, while that of the 2021 image was 26.98 °C. Around 74.7% of the West Bank lands recorded an inverse relationship between the NDVI change and the LST change between 2001 and 2021. Around 25.3% of the West Bank lands recorded a positive relationship. In other words, the study depicted the impact of the NDVI on the LST in the West Bank. The study recommends that policymakers need to increase the green areas in the West Bank to reduce the LST as this is seen to affect the climate conditions in the area.

Keywords: LST; NDVI; West Bank; Palestine; Landsat data.

تحليل تأثير تغيرات معامل الفروق الطبيعية في الغطاء النباتي (NDVI) على درجة حرارة سطح الأرض (LST) باستخدام مرئيات الأقمار الصناعية في الضفة الغربية ، فلسطين

أحمد غيضه

الملخص

بحثت هذه الدراسة في تأثير مؤشر الفروق الطبيعية في الغطاء النباتي (NDVI) على درجة حرارة سطح الأرض (LST) في الضفة الغربية، فلسطين، باستخدام مرئيات الأقمار الصناعية في فترتين زمنيتين. تم استخدام بيانات Landsat 5 TM و Landsat 8 OLI في الدراسة. تم الحصول على بيانات Landsat 5 TM في ٢٩ مارس ٢٠٠١ ، بينما تم الحصول على بيانات Landsat 8 OLI في ٥ أبريل ٢٠٢١. ثم تم حساب NDVI و LST للمرئيتين منهما باستخدام برنامج ArcGIS ١٠,٨. أظهرت نتائج الدراسة أن مؤشر NDVI لمرئية ٢٠٢١ كان أعلى من مرئية عام ٢٠٠١. كان متوسط مؤشر NDVI لمرئية عام ٢٠٠١ حوالي ٠,٢٥، بينما كان لمرئية ٢٠٢١ حوالي ٠,٣٢. بالنسبة إلى درجة حرارة سطح الأرض ، كان متوسط متوسطها لمرئية ٢٠٠١ هو ٢٩,٨٥ درجة مئوية ، بينما كان لمرئية ٢٠٢١ هو ٢٦,٩٨ درجة مئوية. سجل حوالي ٧٤,٧٪ من أراضي الضفة الغربية علاقة عكسية بين تغير NDVI وتغير LST بين عامي ٢٠٠١ و ٢٠٢١. وسجل حوالي ٢٥,٣٪ من أراضي الضفة الغربية علاقة إيجابية. بعبارة أخرى ، شخصت الدراسة تأثير مؤشر NDVI على LST في الضفة الغربية. توصي الدراسة صانعي السياسات في الضفة الغربية بضرورة زيادة المساحات الخضراء من اجل خفض درجة حرارة سطح الأرض نظرا لتأثير ذلك على الظروف المناخية في المنطقة.

الكلمات المفتاحية: درجة حرارة سطح الأرض؛ معامل الفروق الطبيعية في الغطاء النباتي؛ الضفة الغربية؛ فلسطين؛ بيانات لاندسات.

Introduction

Variations of Land Surface Temperature (LST) are mainly decided through land use/land cover type. LST is defined as how hot or cold the Earth's surface feels to the touch (Guillevic et al., 2018). Land use/land cover can be expressed in different ways, one of which is through the NDVI (Aburas et al., 2015). The NDVI describes the difference between the visible and the near infrared reflectance of vegetation cover and can be used to measure the amount and vigor of vegetation on the land surface (Schinasi et al., 2018) The change in the land surface cover from vegetated and moist surfaces to that of an impervious surface is a problem on a global scale (Mallick et al., 2008). The NDVI is used for the mapping of changes in land cover (Lunetta et al., 2006; Singh et al., 2016; Woodcock et al., 2002; Zaitounah et al., 2018). For example, Indrayani et al. (2017) used the NDVI to investigate land cover types in China and Korea.

Applications of the LST have been expanded from simply being used as a climate change indicator to an indicator of plant water stress, drought, land cover/land use changes, urban heat island effects, and so on (Esfandeh et al., 2022; He et al., 2007; Ramaiah et al., 2020).

The analysis of the LST relationship against the NDVI using traditional measurement is time-consuming and costly. Remote sensing technology based on satellite imagery is one of the most effective and efficient alternatives for extracting information from the NDVI and LST changes in an area where it is very difficult to obtain ground observation data in a time series chart (Latha & Rao, 2020; Sarti et al., 2020). The need for remote sensing data in Palestine is crucial because it is difficult to carry out field work under the restrictions of Israeli occupation.

Landsat datasets can be obtained free of charge and can be used for analyzing the LST relationship when the NDVI changes at different geographical levels, be it globally or regionally (Roy et al., 2014; Woodcock et al., 2008). The Landsat 4 and 5 Thematic Mapper (TM), Landsat 7 Enhanced Thematic Mapper + (ETM+), and Landsat 8 Operational Land Imager (OLI), are all able to provide surface reflectance data which can be used to derive NDVI and LST information by using and combining different wavebands. Their capability to provide moderate spatial resolutions (30 m), multispectral images (7, 8, and 11 spectral bands), and time series data, can be used to determine the relationship between NDVI and LST changes. Several vegetation indices can be used for the analysis of land cover or land-use changes, but the NDVI is the most widely used vegetation index approach for the analysis of land cover changes (Xue & Su, 2017). Therefore, the current study used NDVI as an important variable to analyze the LST changes using 2-interval Landsat 5 TM, and Landsat 8 OLI imageries.

Aims of the Study

This paper analyzes the spatial distribution of the LST value in relation to the NDVI or land use/land cover in the West Bank, Palestine. The impact of land cover types based on the NDVI values on the LST was also investigated.

Previous Studies

A number of authors have investigated the impact of the normalized vegetation index, or land cover types on the LST. He et al. (2007) investigated the effect of land use/land cover changes on the change of the urban heat island intensity. The authors found that the urban heat intensity fluctuated throughout China as a result of the land use change. Pal and Ziaul (2017) used multispectral and multitemporal satellite data to detect the impact of land use/land cover on the LST. Results of the study showed that there was an increase in the LST during winter and summer, which was closely attributed to the land cover/land use change. Mallick et al. (2008) used the Landsat 7 ETM+ data to estimate the LST over Delhi. A strong correlation between NDVI and LST over different land cover classes was observed. John et al. (2020) assessed land use/land cover classifications and the LST using multitemporal satellite imagery. The study showed a negative correlation between vegetation land cover and LST. Zaitunah et al. (2018) used multitemporal remote sensing data and GIS technology to quickly detect the NDVI changes. The study showed a substantial change in NDVI values due to extensive human activities in the studied area. Li et al. (2013) reviewed the selected remote sensing algorithms to estimate LST. Trigo et al. (2008) used three sources of data for the LST estimation. They used a SEVIRI onboard Meteosat, MODIS, and ground measurements. Differences with the LST

estimations were observed among the three analyzed sources. Mustafa et al. (2021) investigated the impact of the land use/land cover dynamics and urbanization in Beijing on the LST using multitemporal thermal remote sensing data. The authors found that the considerable increase in the LST was mainly due to urbanization. Liu et al. (2006) used multi remote sensing data sources (ASTER and MODIS) for scaling the LST over a heterogeneous terrain area. Minor differences were found, with a maximum difference of 0.2 K being noted for the upscaled LST. Li et al. (2013) reviewed the status of the selected remote sensing algorithms for the LST estimation using thermal infrared data. The study suggested directions for future research works to improve the accuracy of the estimated LST.

In North West Iran, Feizizadeh et al. (2013) looked at the connection between different land use, land cover types, and LST. The authors discovered an inverse association between the biomass and moisture content and the LST. For the purpose of managing agricultural crop growth and estimating the LST for the Mandya district in India, Aryalekshmi et al. (2020) used the Landsat-8 satellite data. The resulting LST and weather station data were analyzed, and it was discovered that a good agreement existed between the two datasets. Using thermal data from the Landsat 8, previous works were able to create a method for automated LST mapping (Avdan & Jovanovska, 2016). The authors recommended that the technique should be improved with an in-situ LST assessment for future investigations. Tomlinson et al. (2011) reviewed several studies on satellites and sensors, which were useful for LST estimations from the context of meteorology and climatology, such as the study of urban heat islands. Liu et al. (2020) investigated the long-term changes of the LST using three different datasets at a global level. They found that the spatio-temporal of this data fit together very well, and all three sensors showed an uptrend in the annual average of the LST during the long study period (14 years), with considerable spatial variations. The development of the LST reconstruction techniques under hazy situations was evaluated by Mo et al. (2021). They examined five LST reconstruction algorithm techniques. A method for predicting the all-weather 1 km LST using passive microwave and thermal infrared remote sensing data was suggested by Zhong et al. (2021).

Most previous studies have clearly focused on the impact of land use/land cover on the LST at various geographical levels (local, regional, national, and global), whereas this study used the NDVI as a recent trend in addressing this topic at a national geographical level. This study also looked at the elements that influenced the NDVI levels and changes for the two image dates. All previous research, as well as the current study, are concerned about the future of the Earth's environment.

Materials and Methodology

Study area

The West Bank of the River Jordan lies between the latitudes 31° 20′ and 32° 38′ N, and between the longitudes 34° 53′ and 35° 31′ E. Its surface area is 5,860 km².

Figure (1): Location map of the study area (Ghodieh, 2020)

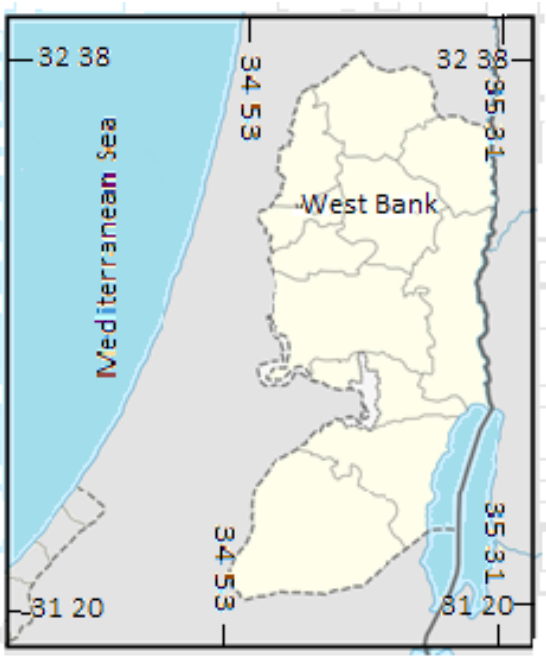

Five climatic zones can be identified in the West Bank, extending from the North to the South (Figure 2): The first region is the Jordan Valley and the Dead Sea. This region is characterized as having a hot and dry summer, and warm winter. The second region is the Eastern slope region, which is characterized by its hot and dry summer, and mild winter. The third region is the semi-arid region, which is characterized by its hot Mediterranean summer and mild winter. The fourth region is the semi-humid region. Its climate is reflec-

tive of a Mediterranean area, being warm in summer and cold in winter. It covers the mountains of the West Bank. The last region is the humid region. This region is close to the Mediterranean Sea, and is characterized by its warm and humid summer, and temperate Mediterranean winter.

The Jordan Valley and the Eastern slope regions receive only between 100-350 mm of rainfall per year, and the annual average temperature is typically between 20-23 °C. The other three climatic regions depict a Mediterranean climate, and receive between 400-700 mm of rainfall per year. The annual average temperature is between 16-18 °C (Applied Research Institute - Jerusalem, 2007).

Figure (2): Climatic regions of the West Bank

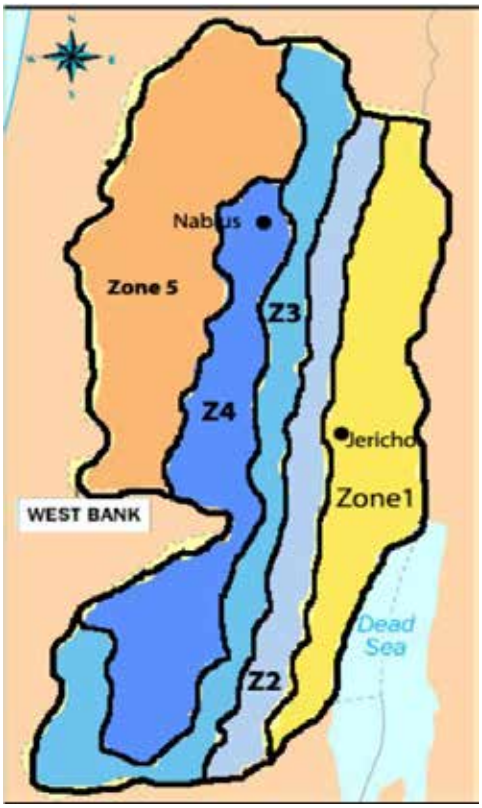

(Alsamamra & Said, 2019)

Topographically, the study area consists of four regions; the semi-coastal region, the mountainous region, the Eastern slope region, and the Jordan Valley region (Hamada & Ghodieh, 2021; see Figure 3).

These physical and climatic features of the West Bank have an impact on both the population distribution and the spatial distribution of the vegetative cover. In comparison to the Eastern slope and the Jordan Valley, the semi-humid and humid regions have thicker vegetative cover. Only the alluvial plains and valleys in the Jordan Valley and Eastern slope regions have vegetation cover. Therefore, rain-fed agriculture is unsuitable in these two regions. The Jordan Valley and the Eastern slope region's agriculture rely on irrigation from groundwater wells.

Figure (3): Topography of the West Bank

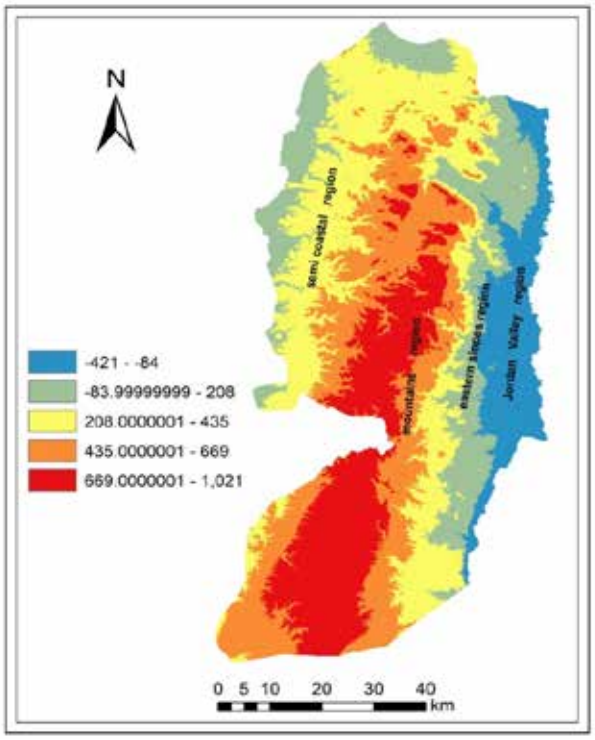

(Hamada & Ghodieh, 2021)

Data sources

Free Landsat 5-TM and Landsat 8-OLI satellite images between the years 2001 and 2021 were downloaded from the USGS website. The equivalent satellite image for the year 2021 was taken on April 5, while the corresponding image for the year 2001 was taken on March 29. This corresponded with the spring season. The spatial resolution of the two images is 30 m. According to the Worldwide Reference System (WRS), the studied area was situated in row 38 and path 174. All datasets were cloud-free, and the two satellite images clearly showed land cover. Sensors from the Landsat 5-TM included the required red and the near infrared wavebands (band 3 and band 4), and one thermal infrared band (band 6). The Landsat-OLI sensors included the red and the near infrared wave bands (band 4 and band 5), and two thermal infrared bands (band 10 and band 11). These wavebands were necessary for the derivation of the NDVI and the LST, respectively. The two satellite images were geo-referenced against the Palestine Grid 1923 system.

Methodology

The USGS website (https://earthexplorer.usgs.gov) provided the satellite data needed for this study. Each image had a size of about 185*185 kilometers. Wavebands from each image were combined into one layer, and clipped to the boundary of the research area (the West Bank) using the ArcGIS-10.8. The spatial resolution of the used wavebands in the study were 30 m, which was appropriate to achieve the objectives of the study (resolution of the thermal infrared bands were resampled to the 30 m value). Additionally, each image's coordinate system was transformed from the Universal Transverse Mercator (UTM) projection to the Palestine Grid 1923.

Driving Land Surface Temperature (LST) and the normalized difference vegetation Index (NDVI) from Landsat 5-TM Data and Landsat 8-TM

To derive the LST from the Landsat 5-TM data and the Landsat 8-OLI, a thermal infrared waveband should exist in the remote sensing system. In Landsat 5-TM, band 6 is noted as the thermal band, and in the Landsat 8-OLI the two thermal bands are denoted by bands 10 and 11. The information for all wavebands including the thermal infrared was stored in the MTL.text file.

The derivation of the LST from the Landsat satellite data can be broken into three steps. First, the raw bands need to be converted into the Top of Atmosphere Radiance (TOAr). Secondly, the TOAr is then converted into degrees Kelvin. Thirdly, the degrees Kelvin is then converted into Celsius or Fahrenheit (Khan et al., 2021; Lamare et al., 2020; Spampinato et al., 2011).

To calculate the at-satellite brightness temperature, the following equation can be used (https://www.usgs.gov):

$$T = \frac{k2}{\ln\left(\frac{k1}{L\lambda} + 1\right)} \ldots\ldots \text{Equation1}$$

Where:

T = Top of atmosphere brightness temperature (K)
L_λ = TOA spectral radiance (Watts/(m2 * srad * μm))
K_1 = Band-specific thermal conversion constant from the metadata (K1_CONSTANT_BAND_thermal band)
K_2 = Band-specific thermal conversion constant from the metadata (K2_CONSTANT_BAND_6, where 6 is the thermal band number)

For the thermal band (band 6) of the Landsat 5-TM, the k1 and k2 values are as follows:

K1 = 607.76, k2 = 1260.56

For the thermal bands (10 and 11) of the Landsat 8 –OLI, the k1 and k2 are as follows:

K1_CONSTANT_BAND_10 = 774.8853

K2_CONSTANT_BAND_10 = 1321.0789

K1_CONSTANT_BAND_11 = 480.8883

K2_CONSTANT_BAND_11 = 1201.1442

TOAr = ((LMAX - LMIN) / (CALMAX - CALMIN))*(Thermal BAND - CALMIN) + LMIN….Equation 2

The results of Equation 2 were used in Equation 3 to derive the LST in Kelvin.

The conversion of the TOAr to the Brightness Temperature (BT) is as follows:

BT (Kelvin) = k2 / Ln (K1 / TOAr layer + 1) …. Equation 3

The resultant layer of Equation 3 can be used in Equation 4 to convert the Kelvin measurement unit into the Celsius unit.

To understand the impact of the NDVI on the LST of the West Bank for the two image dates, the NDVI was estimated using the red (R) and the near-infrared wavebands (NIR), as shown in Equation 7. The NDVI values ranged between -1 and +1, where values below 0.1 represented the water and vegetation-free surfaces, while the values above 0.1 represented the surfaces with different percentages of vegetation cover.

Before the NDVI estimation, the ToA was first calculated because the Surface Reflectance (SR) estimation is the most critical pre-processing step for deriving the geophysical parameters in a multi-sensor remote sensing work (Bilal et al., 2019). The spectral radiance data was converted into the planetary ToA using the coefficients of reflectance rescaling available in the files. For converting DN values into ToA, the reflection values were substituted in the following equation:

ρλ' = M ρQcal + A ρ …… Equation 5

Where M is the band-specific multiplicative rescaling factor from the metadata, A is the band-specific additive rescaling factor from the metadata, Qcal is the quantized and calibrated standard product pixel values, and ρλ' is the ToA planetary reflectance without correction for the solar angle (DN).

To reduce the effect of the sun's elevation, the reflec-

tance values of the two images with the sun's angle were corrected using the following equation:

$$\rho\lambda = \rho\lambda' / \sin \theta SE \quad \text{..... Equation 6}$$

Where, ρλ is the ToA planetary reflectance, and θSE is the local sun's elevation angle. The scene center sun elevation angle in degrees is provided in the metadata of the image (sun's elevation).

At this stage, the Landsat 5-TM and the Landsat 8-OLI images were ready for the NDVI calculation:

$$NDVI = (NIR - R) / (NIR + R) \quad \text{..... Equation 7}$$

Results and Discussion

The Equal Interval Method (EIM) for LST mapping was adopted. The temperature maps were divided into five temperature classes.

LST and NDVI from the Landsat 5-TM satellite data on March 29, 2001

Figure 4 shows the LST of the West Bank. It ranges from 10 °C to 45 °C. However, the first and the last LST classes (10 to 17 & 38 to 45 °C) represent less than 1% of the West Bank. Therefore, they can be excluded from the analysis. The high LST values were concentrated in the eastern half of the West Bank, which represents the Eastern slope region, and the Jordan Valley and the Dead Sea region, or the arid and semi-arid regions. On the other hand, the relatively low LST was mainly concentrated in the western half of the West Bank, which represents the humid and semi-humid regions (Mediterranean regions).

Figure (4): Land surface temperature, LST (°C) of the West Bank on March 29, 2001

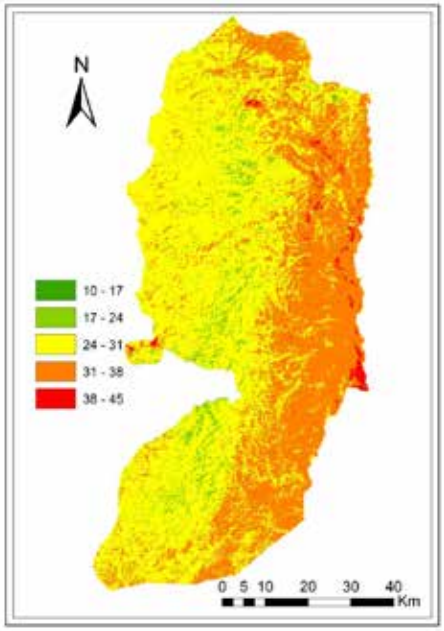

The surf is calculated using the following formula:

Area = count * 30 m * 30 m / 1,000,000 m²

Where the count represents the number of pixels of the LST class, 30 m is the pixel size, and 1,000,000 is equivalent to one km². Table 1 shows the LST area for each class.

Table 1 shows that the LST of about 94% of the West Bank was between 24 and 38 °C. Almost 5% of the LST area was between 17 and 24 °C. Additionally, 1% of the LST area was between 38 and 45 °C, and a very small area (0.5 km²) had a LST between 10 and 17 °C. Geographically, 65.85% of the West Bank had an LST between 10 to 31 °C, which belongs to the Mediterranean climatic region, while 34.15% had a LST between 31 and 45 °C, which belongs to the arid and the semi-arid climatic regions.

Table (1): Area of the LST of the West Bank for each class on March 29, 2001

LST class (C°)	Area (km²)	Area (%)
17-10	0.5067	0.00
24-17	278.3403	4.92
31-24	3,446.2860	60.93
38-31	1,877.6750	33.20
45-38	53.4276	0.95
	5,656.2356	100

The NDVI map is divided into five classes based of the thematic meaning of each class in terms of land use/ land cover type. The reference NDVI values were used to describe each class, as shown in Table 2.

Table (2): Reference values used for the reclassification of the NDVI values for the two image dates

	NDVI value	Description of class
1	-1.000 to 0.000	Water and moist soil
2	0.000 to 0.100	Bare soil and rocks
3	0.100 to 0.200	Sparse green vegetation cover
4	0.200 to 0.600	Moderate-to-dense green vegetation cover
5	>0.600	Dense green vegetation cover

Figure (5): Normalized difference vegetation index

of the West Bank on March 29, 2001

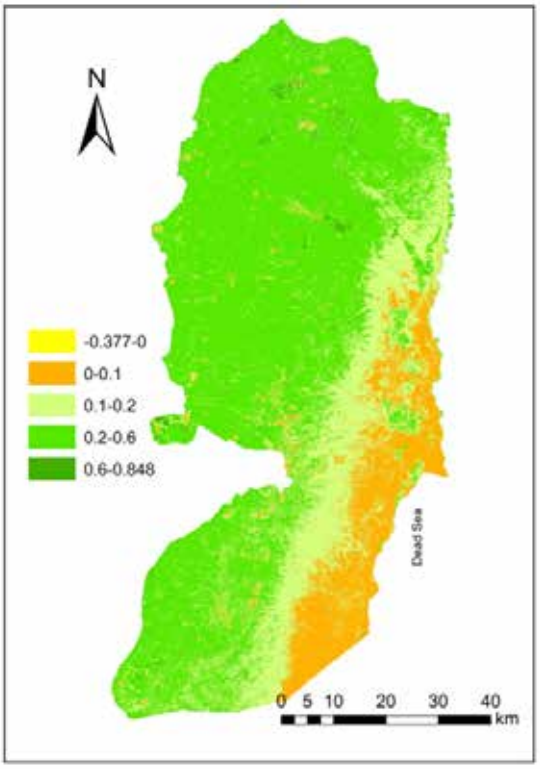

Figure 5 shows that the negative values of the NDVI were represented by water and moist soil land cover. This was limited to a small area in the mid-north of the West Bank. This class represented only 1.154 km² (Table 3). The bare soil and rocks classes with NDVI values were between 0 and 0.1 and were concentrated around the Dead Sea and the southern part of the Jordan Valley, in addition to the urban built-up areas. This class occupies 742.12 km² or 13.12% of the West Bank and receives an average of less than 200 mm of annual rainfall.

The NDVI of the third class was between 0.1 and 0.2, and represented the sparse vegetation land cover. This class covered 1,293.185 km² or 22.87% of the West Bank. It covers the upper parts of the Eastern slope region, which receives around 300 mm of rainfall per year. It is mostly used for grazing. Areas with the NDVI between 0.2 and 0.6 represent moderate to dense green vegetation and cover 3,553.194 km² or 62.83%. This class covers the semi-humid and the humid climatic regions (the Mediterranean regions), and receives between 400 to 700 mm of rainfall per year. It is mainly covered with olive and fruit trees. The NDVI of the last class was between 0.6 and 0.848 and represents lands with dense green vegetation. It covers only 66.60 km² or 1.18% of the West Bank. This class is concentrated in the northern plains which are planted with vegetables and crops, and the broadleaf forests in the north-western part of the West Bank. The area of each class was calculated using the same formula for the LST class area estimation. Table 3 shows the NDVI area for each class.

Table (3): Area estimation of the NDVI classes for the image acquired on March 29, 2001

	NDVI class value	Description	Area (km²)	%
1	-0.377 to 0.000	Water and moist soil	1.15	0.00
2	0.000 to 0.100	Bare soil and rocks	732.00	13.12
3	0.100 to 0.2000	Sparse green vegetation cover	1,295.02	22.87
4	0.200 to 0.600	Moderate-to-dense vegetation cover	3,561.49	62.83
5	0.600 to 0.848	Dense vegetation cover	66.58	1.18
		Total	5,656.24	100

Impact of NDVI on the LST from March 29, 2001

To identify the impact of the NDVI on the LST, the LST map and the NDVI map were converted into polygons. Subsequently, two vector layers were overlaid using the ArcGIS 10.8.A cross matrix of the LST and NDVI, including the intersected areas between each class and the other classes. Table 4 shows the results of the intersection process between the two maps.

Table (4): Intersection area of the NDVI values and the

LST values for the Landsat 5-TM image on March 29, 2001

NDVI / LST C°	-0.3776 to 0.0 Water and moist soil	0.0 to 0.1 Bare soil and rocks	0.1 to 0.2 Sparse green vegetation cover	0.2 to 0.6 Moderate to dense green vegetation cover	0.6 to 0.8477 Dense green vegetation cover	Area (km²)** and %
10 to 17	616 m²*	0.183	0.201	0.108	0.0	0.4926 0.00%
17 to 24	0.436	12.921	29.030	226.5305	7.769	276.6865 4.89%
24 to 31	0.475	172.543	505.147	2,723.95	51.504	3,453.619 61.06%
31 to 38	0.135	521.850	736.981	606.399	7.290	1,872.655 33.12%
38 to 45	0.101	24.499	23.691	4.495	719 m²*	52.787 0.93%
Total	1.15 0.02%	732.00 12.94%	1,295.02 22.90	3,561.49 62.97%	66.58 1.18%	5,656.24

* very small area
** detailed areas are slightly changed after data conversion from raster to polygon

Table 4 shows that the first and the last temperature classes (10 to 17 °C and 38 to 45 °C) can be excluded from the analysis because they represent only 616 m² (0%) and 52.787 km² (less than 1%), respectively. The table also shows that the largest area is represented by the temperature class 24 to 31 °C. This class represents 3,453.619 km² or 61% of the West Bank. About 69% of this class area lies in the moderate to dense green vegetation cover, 1.5% lies in the dense vegetation class, 14.6% lies in the sparse green vegetation class, and about 5% lies in the bare soil and rocks class. Geographically, this class covers the mountains and the western slopes of the West Bank, or the semi-humid and humid climatic regions, in addition to a small part of the upper eastern slopes. The second largest area is represented by the temperature class 31 to 38 °C. It covers 1,872.655 m² or 33% of the West Bank. This area is distributed into three NDVI classes: the bare soil and rocks (28%), sparse green vegetation (39%), and moderate to dense green vegetation (32%). Geographically, this class covers the lower eastern slopes of the West Bank, or the semi-arid region. Unmanaged grass is the dominant land cover in this area, and is mainly used for grazing. The last LST class was 17 to 24 °C. It covers 276.6865 km² or 5% of the West Bank. About 85% of this class lies in the moderate and dense green vegetation classes, 10% lies in the sparse vegetation cover class, and 5% lies in the bare soil and rocks class. Geographically, it covers the middle and high mountainous lands which are covered with forests, bushes, unmanaged grass, and olive trees (Figure 6).

Figure (6): An example of moderate to dense green vegetation cover in the high mountains of the West Bank with relatively low LST (17-24 C°)

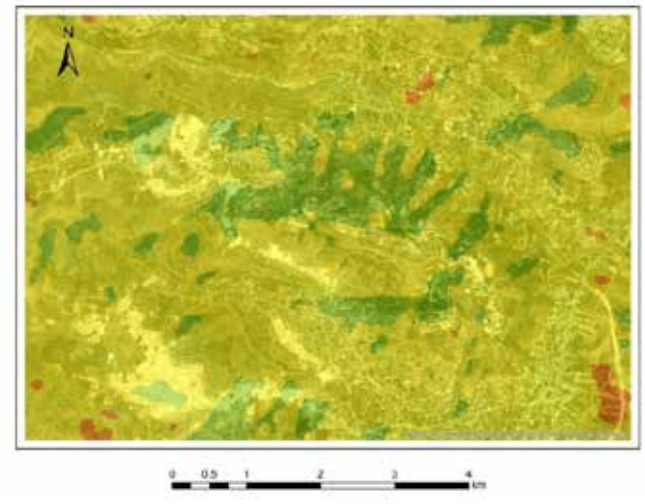

A correlation matrix using the Pearson correlation coefficient between the land cover classes based on the NDVI values and the LST was conducted. The center of the NDVI and the LST classes was used. Table 5 shows the correlation between the land cover type and the LST.

Table (5): Correlation coefficient between NDVI (land cover) and LST in the West Bank from the image of March 29, 2001

Land cover	LST
Water and moist soil	-0.074
Bare soil and rocks	0.399
Sparse green vegetation cover	0.350
Moderate to dense green vegetation	0.053
Dense green vegetation	-0.003

Table 5 shows that the moist soils (NDVI = -0.3776 to 0.0) have a negative correlation with the LST (10-17 °C), which means that areas with water and moist soils have a low LST. This class was limited to a very small area in the northern West Bank. Bare soil and rocky areas (NDVI = 0.0-0.1) had a positive correlation with the LST (31-38 °C), which meant that the surfaces which were free of vegetation had a relatively higher temperature. Also, areas with sparse vegetation or a low NDVI (0.1-0.2) had a positive correlation with the LST (24-31 °C and 31-38 °C), which means that the surfaces with sparse vegetation also have a relatively higher temperature. Surfaces with moderate to dense vegetation (NDVI = 0.2-0.6) have almost no correlation with the LST, because these surfaces are a mixture of vegetation, soil, and rocks. Therefore, the LST of these surfaces is moderate (24-31 °C). On the other hand, the dense vegetation surfaces (NDVI > 0.6) have a negative correlation with the LST, which means that the higher the NDVI, the lower the LST. The LST of these surfaces were mostly between 24-31 °C.

LST and NDVI of the Landsat 8-OLI satellite data from April 5, 2021

Figure 7 demonstrates that on April 5, 2021, the West Bank's LST varied between 16 to 39 ^{o}C. In the lower Eastern slope region, i.e., the Jordan Valley, the Dead Sea region, or the dry region, relatively higher LST values were noted. The comparatively low LST, on the other hand, was primarily found in the northern West Bank and in the high hilly regions, which characterize the semi-humid Mediterranean region. The upper eastern slopes as well as the semi-coastal or humid regions had moderate LST values.

Figure (7): LST (^{o}C) of the West Bank on April 05, 2021

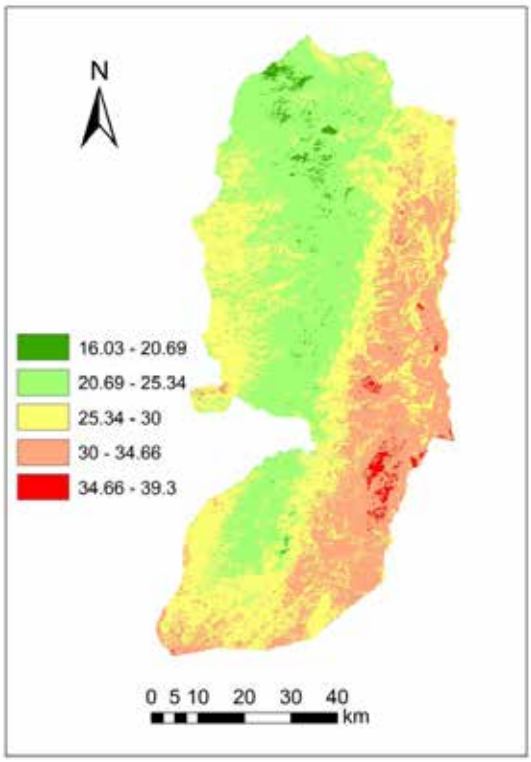

Table (6): Area of LST of the West Bank for each class on April 05, 2021

LST class (C°)	Area (km²)	Area (%)
16.03-20.69	66.205	1.17
20.69-25.34	2,125.904	37.59
25.34-30.00	2,062.592	36.47
30.00-34.66	1,356.042	23.97
34.66-39.30	45.493	0.8
Total	5,656.24	100

Table 6 shows that the first and the last LST classes represented a small percentage of the West Bank area (1.8%). This was shared with the image from 2001. It also shows that the Mediterranean regions covered 75.23% of the LST between 16.03 and 30.00 ^{o}C, while the semi-arid and arid regions covered 24.77% of the study area with LST between 30 and 39 ^{o}C.

The NDVI map from April 05, 2021, was also divided into five classes based on the thematic meaning of each class in terms of land use /land cover type (Figure 8). The same reference NDVI values shown in Table 2 were used to describe each class.

Figure (8): Normalized difference vegetation index of the West Bank on April 05, 2001

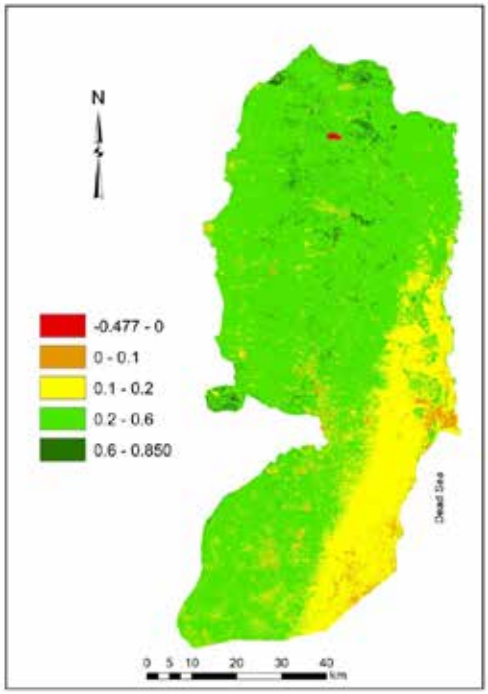

Figure 8 shows good NDVI values for most of the West Bank on April 05, 2021. More than 75% of the West Bank was covered with moderate to dense and dense vegetation. Only 2.03% was without vegetation cover (bare soil and rocks including urban areas and moist soil). A total of 22.47% was a mixture of vegetation and bare soil and rocks.

Table (7): Area estimation of NDVI classes for the image acquired on April 05, 2021

	NDVI class value	Description	Area (km²)	%
1	-0.477 to 0.000	Water and moist soil	5.6864	0.10
2	0.000 to 0.100	Bare soil and rocks	109.0130	1.93
3	0.100 to 0.2000	Sparse green vegetation cover	1,261.9572	22.30
4	0.200 to 0.600	Moder-ate-to-dense vegetation cover	4,127.9901	72.99
5	0.600 to 0.850	Dense vegeta-tion cover	151.6967	2.68
		Total	5,656.24	100

Impact of NDVI on LST on April 05, 2021

In order to identify the impact of NDVI on the LST from the image in 2021, the same process was used for the image from 2001 was repeated. The two maps were overlaid after being converted into a polygon, and the intersected area of the two map classes was calculated. Table 8 shows the intersection results of the NDVI classes and the LST classes.

Table (8): Intersection area of NDVI values and LST values for the Landsat 8-OLI image on April 05, 2021

NDVI / LST C°	-0.3776 to 0.0 Water and moist soil	0.0 to 0.1 Bare soil and rocks	0.1 to 0.2 Sparse green vegetation cover	0.2 to 0.6 Moderate to dense green vegetation cover	0.6 to 0.8477 Dense green vegetation cover	Area (km²)** and %
16.03 to 20.69	3.5233	2.0936	2.8531	43.6941	14.0409	66.205 1.17%
20.69 to 25.34	1.2034	23.8209	113.3091	1,874.4206	113.1500	2,125.904 37.59%
25.34 to 30.00	0.6322	33.2352	292.9820	1,711.4617	24.2906	2,062.592 36.47%
30.00 to 34.66	0.1275	49.2391	812.3389	493.1394	0.1751	1,356.042 23.97%
34.66 to 39.30	0.0044	0.6202	39.7341	5.1343	0.00	45.493 0.80%
Total	5.4908 0.10%	109.009 1.93%	1,261.2172 22.30%	4,127.8501 72.99%	151.6566 2.68%	5,656.24

** detailed areas are slightly changed after data conversion from raster to polygon.

Table 8 shows that 87.2% of the temperature ranged between 16.03 to 20.69 ^{o}C of the LST class which was covered with moderate to dense and dense vegetation. Around 87% of the temperature range between 34.66 to 39.3 ^{o}C, and 20.69 to 30.0 ^{o}C of the LST class was covered with sparse green vegetation. Also, 75% of the dense green vegetation lay in the 20.69 to 25.34 ^{o}C LST class, and 75% of the bare soil and rocks lay in the 25.34 to 30.0^{o}C and 30.0 to 34.66^{o}C LST classes. The relationship between the NDVI values (land cover types) and LST values were investigated using Pearson's Correlation (Table 9).

Table (9): Person Correlation coefficient between NDVI (land cover) and LST in the West Bank from the image on April 05, 2021

Land cover	LST
Water and moist soil	-0.893
Bare soil and rocks	0.171
Sparse green vegetation cover	0.368
Moderate to dense green vegetation	-0.255
Dense green vegetation	-0.424

Table 9 shows a strong negative correlation between water and moist soil land cover with the LST, and a negative correlation between moderate and dense vegetation cover with LST. In addition, a positive correlation was noted between the bare soil and sparse vegetation land cover with the LST. The sparse vegetation cover class was mostly covered with rocks and bare soil, and the correlation between these two classes was 0.904. This means that the greater the density of vegetation cover and soil moisture content, the lower the surface temperature of the land.

Comparison of NDVI and LST between 2001 and 2021

Analysis of the NDVI values from the two image dates showed that the NDVI values from the 2021 image was higher than that of spring 2001. The average NDVI from 2021 in the West Bank was 0.32 with a standard deviation of 0.15, while that of spring 2001 was 0.25 with a standard deviation of 0.13. This affected the LST of the two images. The average LST in 2001 was about 29.85 ^{o}C, and in 2021 it reached about 26.98 ^{o}C (Table 10).

Table (10): Statistical characteristics of the West Bank NDVI and LST

	Image of Spring 2001	Image of Spring 2021
NDVI mean	0.25	0.32
NDVI standard deviation	0.13	0.15
LST mean C°	29.85	26.98
LST standard deviation C°	3.57	3.56

NDVI change between 2001 and 2021

Using the raster calculator in the ArcGIS 10.8 version, the NDVI values for the year 2001 were subtracted from that of the year 2021. A new map was produced, which represented the positive and the negative NDVI differences between the two image sets (Figure 9).

Figure (9): NDVI change between the years 2001 and 2021

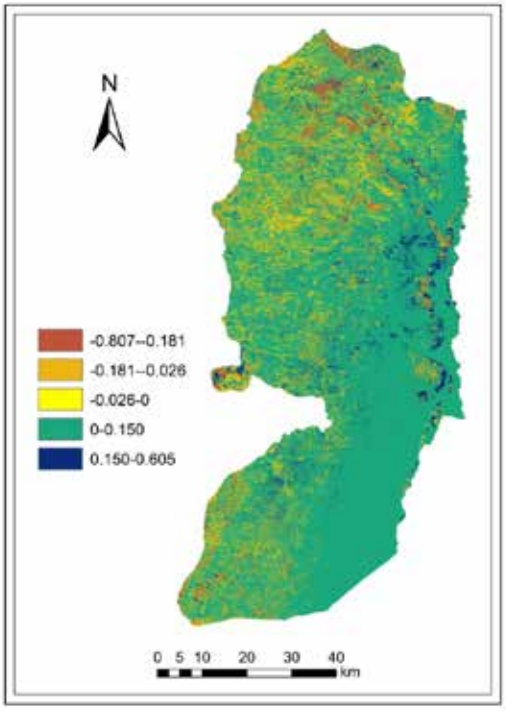

Table (11): NDVI change between the years 2001 and 2021

	Class	Area (km^2)	Percentage
1	-0.800- -0.181	139.518	2.47
2	-0.18- -0.026	694.846	12.28
3	-0.026-0.000	351.415	6.21
4	0.000-0.150	4,184.486	73.98
5	0.150-0.605	285.999	5.06
		5,656.24	100

In order to identify the NDVI change more clearly, the NDVI change map was reclassified into two classes. The first one represented the negative change, and the other represented the positive change (Figure 10 and Table 12).

Figure (10): Negative and positive NDVI change

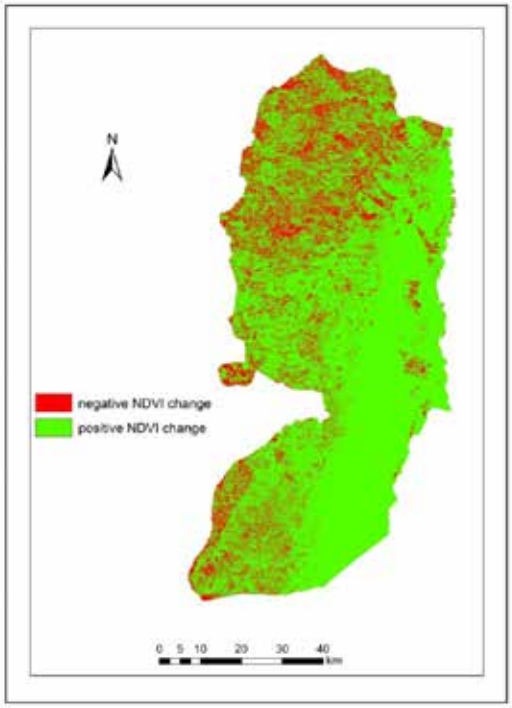

Table (12): Negative and positive NDVI change

Change	Area (km²)	Percentage
Negative	1,185.779	20.96
Positive	4,470.457	79.04
	5,656.24	100

Figures 9 and 10 and Tables 11, 12 show that about 80% of the West Bank had a positive change in the NDVI between 2001 and 2021, while about 20% had a negative change. This was due to the higher average rainfall in the year 2021 by around 35%. This was especially true in the northern half of the West Bank (Palestine Central Bureau of Statistics, 2005).

LST change between the years 2001 and 2021

Using the raster calculator in the ArcGIS 10.8 version, the LST values for the year 2001 were subtracted from that of the year 2021. A new map was produced representing the positive and the negative LST differences between the two image sets (Figure 11).

Figure (11): LST change between the years 2001 and 2021

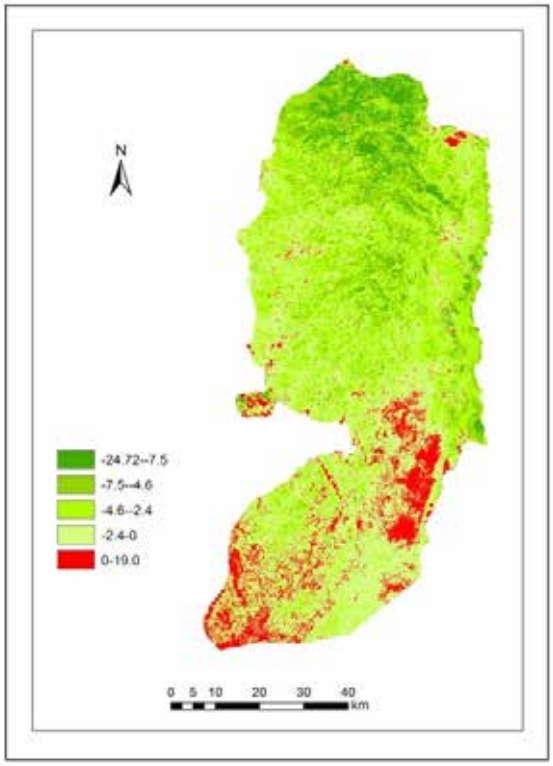

To identify the LST change much more clearly, the LST change map was reclassified into two classes. One represented the negative change, and the other represented the positive change (Figure 12 and Table 13).

Figure (12): Negative and positive NDVI change

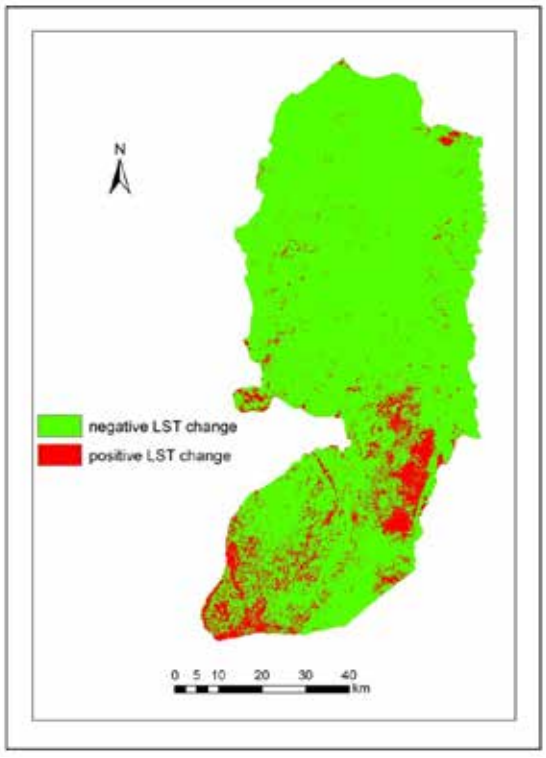

Table (14): Negative and positive LST change

Change	Area (km²)	Percentage
Negative	5,070.695	89.65
Positive	585.540	10.35
	5,656.24	100

Figures 11 and 12 and Tables 12 and 13 show that about 90% of the West Bank had a negative change in the LST between 2001 and 2021, while about 10% had a positive change. This was mainly due to the denser greener vegetation or higher NDVI for the year 2021, especially in the northern half of the West Bank.

In order to understand the relationship between the NDVI change and the LST change (negative and positive change maps), the two maps were converted from raster to polygon, and then overlaid using the intersect geoprocessing function in the ArcGIS software. Results of intersection process are shown in Table 14.

Table (14): Results of intersection process between the NDVI and the LST change maps (km²)

	Negative LST change	Positive LST change
Negative NDVI change	1,003.402 (17.7%)	4,070.567 (72.0%)
Positive NDVI change	152.116 (2.7%)	428.987 (7.6%)

Table 14 shows that 72% of the lands with a negative NDVI change were overlapped with lands having a positive LST change (inverse relationship), while 17.7% had a positive relationship. On the other hand, 2.7% of the positive NDVI change was overlapped with the negative LST change (inverse relationship), while 7.6% had a positive relationship. In other words, 74.7% of the lands had an inverse relationship between the NDVI and the LST, while 25.3% had a positive relationship in the spring season.

Conclusion

The temporal changes in NDVI and LST in the West Bank, Palestine, during 2001 and 2021 were analyzed in this study. Results showed that the mean NDVI in the study area increased from 0.25 in 2001, to 0.32 in 2021. This increase in the NDVI values was mainly due to the higher amount of rainfall in 2021 compared to that of 2001, by around 35%, particularly in the northern mountains of the West Bank. The results also showed a considerable decrease in the LST from 29.85 ^{o}C in 2001 to 26.98 ^{o}C in 2021 (-2.87 ^{o}C change). About 90% of the study area recorded a negative LST change between 2001 and 2021. Also, an inverse relationship was recorded between the NDVI values and the LST values for 74.7% of the West Bank lands. The negative change of the LST was concentrated in the high lands and the eastern slopes of the West Bank. These areas recorded higher NDVI values.

The study recommended that future research could increase the credibility of the obtained results by incorporating ground truthing. Also, future studies could use other vegetation indices such as SAVI, TSAVI, MSAVI, DVI, and GNDVI, to evaluate their effectiveness in capturing vegetation changes. Advanced techniques like genetic programming, soft computing, and deep learning can also be explored in future studies to synthesize and combine spectral bands to derive more robust vegetation indices

References

Aburas, M., Abdullah, S. H., Ramli, M. F., & Asha'ari, Z. H. (2015, August 19-20). Land cover change using NDVI Index [Poster presentation]. International Conference on Environmental Forensics 2015 (iENFORCE2015), Putrajaya, Malaysia. https://doi.org/10.13140/RG.2.1.4021.0000

Alsamamra, H., & Said, N. (2019). An overview of green buildings potential in Palestine. International Journal of Sustainable and Green Energy, 8(2), 20-33.

Applied Research Institute - Jerusalem (ARIJ). (2007). Status of the environment in the Occupied Palestinian Territory. https://www.arij.org/wp-content/uploads/2013/12/2007_Status_of_Environment.pdf

Aryalekshmi, B. N., Biradar, R. C., & Chandrasekar, K. (2020). Land surface temperature estimation of Mandya district using LANDSAT-8 data. Journal of Applied Science and Engineering, 23(4), 583-591.

Avdan, U., & Jovanovska, G. (2016). Algorithm for automated mapping of land surface temperature using LANDSAT 8 satellite data. Journal of Sensors, 2016. https://doi.org/10.1155/2016/1480307

Bilal, M., Nazeer, M., Nichol, J. E., Bleiweiss, M. O., Qiu, Z., Jäkel, E. … Lolli, X.. (2019). A simplified and robust Surface Reflectance Estimation Method (SREM) for use over diverse land surfaces using multi-sensor data. Remote Sensing, 11(11), 1344. https://doi.org/10.3390/rs11111344

Esfandeh, S., Danehkar, A., Salmanmahiny, A., Sadeghi, S.M. M., & Marcu, M. V. (2022). Climate change risk of urban growth and land use/land cover conversion: An in-depth review of the recent research in Iran. Sustainability, 14, 338. https://doi.org/10.3390/su14010338

Feizizadeh, B., Blaschke, T., Nazmfar, H., Akbari, E., & Kohbanani, H. R. (2013). Monitoring land surface temperature relationship to land use/land cover from satellite imagery in Maraqeh County, Iran. Journal of Environmental Planning and Management, 56(9), 1290-1315.

Ghodieh, A. (2020). Urban built-up area estimation and change detection of the Occupied West Bank, Palestine, using multi-temporal aerial photographs and satellite images. Journal of the Indian Society of Remote Sensing, 48, 235-247. https://doi.org/10.1007/s12524-019-01073-8

Guillevic, P., Göttsche, F., Nickeson, J., Hulley, G., Ghent, D., Yu, Y., ... & Camacho, F. (2018). Land surface temperature product validation best practice protocol. Version 1.1. In P. Guillevic, F. Göttsche, J. Nickeson & M. Román (Eds.), Good practices for satellite-derived land product validation (p. 58). Land Product Validation Subgroup (WGCV/CEOS). https://doi.org/10.5067/doc/ceoswgcv/lpv/lst.001

Hamada, S., & Ghodieh, A. (2021). Mapping of solar energy potential in the West Bank, Palestine using Geographic Information Systems. Papers in Applied Geography, 7(3), 256-273.

He, J. F., Liu, J. Y., Zhuang, D. F., Zhang, W., & Liu, M. L. (2007). Assessing the effect of land use/land cover change on the change of urban heat island intensity. Theoretical and Applied Climatology, 90(3), 217-226.

https://www.pcbs.gov.ps/Downloads/book1143.pdf

Indrayani, E., Buchari, A., Putranto, D.D. A., & Saleh, E. (2017). Analysis of land use in the Banyuasin district using the image Landsat 8 by NDVI method. AIP Conference Proceedings, 1903, p. 030007. https://doi.org/10.1063/1.5011514

John, J., Bindu, G., Srimuruganandam, B., Wadhwa, A., & Rajan, P. (2020). Land use/land cover and land surface temperature analysis in Wayanad district, India, using satellite imagery. Annals of GIS, 26(4), 343-360. https://doi.org/10.1080/19475683.2020.1733662

Khan, A., Chatterjee, S., & Weng, Y. (2021). 2-characterizing thermal fields and evaluating UHI effects. In A. Khan, S. Chatterjee, & Y. Weng (Eds.),

Urban heat island modeling for tropical climates (pp. 37-67). Elsevier.

Lamare, M., Dumont, M., Picard, G., Larue, F., Tuzet, F., Delcourt, C., & Arnaud, L. (2020). Simulating optical top-of-atmosphere radiance satellite images over snow-covered rugged terrain. The Cryosphere, 14(11), 3995-4020.

Latha, P. S., & Rao, K. N. (2020). Assessment of land use and land cover changes (1988-2020) through NDVI analysis and geospatial techniques. International Journal of Research and Review, 7(12), 549-559.

Li, Z. L., Tang, B. H., Wu, H., Ren, H., Yan, G., Wan, Z., ... & Sobrino, J. A. (2013). Satellite-derived land surface temperature: Current status and perspectives. Remote Sensing of Environment, 131, 14-37.

Liu, J., Hagan, D. F. T., & Liu, Y. (2020). Global land surface temperature change (2003-2017) and its relationship with climate drivers: AIRS, MODIS, and ERA5-land based analysis. Remote Sensing, 13(1), 44. https://doi.org/10.3390/rs13010044

Liu, Y., Hiyama, T., & Yamaguchi, Y. (2006). Scaling of land surface temperature using satellite data: A case examination on ASTER and MODIS products over a heterogeneous terrain area. Remote Sensing of Environment, 105(2), 115-128.

Lunetta, R. S., Knight, J. F., Ediriwickrema, J., Lyon, J. G., and Worthy, L. D. (2006). Land-cover change detection using multi-temporal MODIS NDVI data. Remote Sensing of Environment, 105(2), 142-154.

Mallick, J., Kant, Y., & Bharath, B. D. (2008). Estimation of land surface temperature over Delhi using Landsat-7 ETM+. The Journal of Indian Geophysical Union, 12(3), 131-140.

Mo, Y., Xu, Y., Chen, H., & Zhu, S. (2021). A review of reconstructing remotely sensed land surface temperature under cloudy conditions. Remote Sensing, 13(14), 2838.

Mustafa, E. K., Liu, G., Abd El-Hamid, H. T., & Kaloop, M. R. (2021). Simulation of land use dynamics and impact on land surface temperature using satellite data. GeoJournal, 86, 1089-1107. https://doi.org/10.1007/s10708-019-10115-0

Pal, S., & Ziaul, S. K. (2017). Detection of land use and land cover change and land surface temperature in English Bazar urban center. The Egyptian Journal of Remote Sensing and Space Sciences, 20, 125-145.

Palestine Central Bureau of Statistics. (2005). Meteorological conditions in the Palestinian Territory, annual report 2004.

Ramaiah, M., Avtar, R., & Rahman, M. (2020). Land cover influences on LST in two proposed smart cities of India: Comparative analysis using spectral indices. Land, 9(9), 292. https://doi.org/10.3390/land9090292

Roy, D. P., Qin, Y., Kovalskyy, V., Vermote, E. F., Ju, J., Egorov, A., ... & Yan, L. (2014). Conterminous United States demonstration and characterization of MODIS-based Landsat ETM+ atmospheric correction. Remote Sensing of Environment, 140, 433-449.

Sarti, M., Vaccari, F. P., Calfapietra, C., Brugnoli, E., & Scartazza, A. (2020). A statistical approach to detect land cover changes in Mediterranean ecosystems using multi-temporal Landsat data: The case study of Pianosa Island, Italy. Forests, 11(3), 334. https://doi.org/10.3390/f11030334

Schinasi, L. H., Benmarhnia, T., & De Roos, A. J. (2018). Modification of the association between high ambient temperature and health by urban microclimate indicators: A systematic review and meta-analysis. Environmental Research, 161, 168-180.

Singh, R. P., Singh, N., Singh, S., & Mukherjee, S. (2016). Normalized difference vegetation index (NDVI) based classification to assess the change in land use/land cover (LULC) in Lower Assam, India. International Journal of Advanced Remote Sensing and GIS, 5(10), 1963-1970.

Spampinato, L., Calvari, S., Oppenheimer, C., & Boschi, E. (2011). Volcano surveillance using infrared cameras. Earth-Science Reviews, 106(1-2), 63-91.

Tomlinson, C. J., Chapman, L., Thornes, J. E., & Baker, C. (2011). Remote sensing land surface temperature for meteorology and climatology: A review. Meteorological Applications, 18(3), 296-306.

Trigo, I. F., Monteiro, I. T., Olesen, F., & Kabsch, E. (2008). An assessment of remotely sensed land surface temperature. Journal of Geophysical Research: Atmospheres, 113(D17). https://doi.org/10.1029/2008JD010035

Woodcock, C. E., Allen, R., Anderson, M., Belward, A., Bindschadler, R., Cohen, W., ... & Wulder, M.A. W. (2008). Free access to Landsat imagery. Science, 320(5879), 1011. https://doi.org/10.1126/science.320.5879.1011a

Woodcock, C. E., Macomber, S. A., & Kumar, L. (2002): Vegetation mapping and monitoring. In A. K. Skidmore (Ed.), Environmental modelling with GIS and Remote Sensing (pp. 97-120). Taylor and Francis.

Xue, J., & Su, B. (2017). Significant remote sensing vegetation indices: A review of developments and applications. Journal of Sensors, 2017, 1-17. https://doi.org/10.1155/2017/1353691.

Zaitunah, A., Samsuri, Ahmad, A. G., & Safitri, R. A. (2018). Normalized difference vegetation index (ndvi) analysis for land cover types using landsat 8 oli in besitang watershed, Indonesia. IOP Conference Series: Earth and Environmental Science, 126(2018), 012112. https://doi.org/10.1088/1755-1315/126/1/012112

Zhong, Y., Meng, L., Wei, Z., Yang, J., Song, W., & Basir, M. (2021). Retrieval of all-weather 1 km land surface temperature from combined MODIS and AMSR2 data over the Tibetan Plateau. Remote Sensing, 13(22), 4574. https://doi.org/10.3390/rs13224574